SPECIAL COMMUNICATION

Initial on-Orbit Results from the GOES-18 Spacecraft Science Magnetometer

Paul T.M. Loto'aniu[1,2] · A. Davis[1,2] · A. Jarvis[1,2] · M. Grotenhuis[3] · F.J. Rich[4] · S. Califf[1,2] · F. Inceoglu[1,2] · A. Pacini[2] · H.J. Singer[5]

Abstract

The Geostationary Operational Environmental Satellite (GOES)-18, the latest spacecraft from the NOAA GOES-R satellite series, was launched March 1, 2022. As with the previous GOES-16 and GOES-17 satellites, GOES-18 monitors sources of space weather on the Sun and its effects at Earth. NOAA uses GOES data as part of the national space weather forecasts, warnings and alerts to many customers. GOES-18 hosts new magnetometers called the Goddard magnetometers (GMAG) that replace those (called MAG) built by a different vendor on GOES-16 and GOES-17. Like the other GOES satellites, the GOES-18 GMAG provides observations of the geomagnetic field at geostationary orbit (35,786 km), a location that often provides early indication of enhanced space weather activity. In this paper, we review the capabilities of the GOES-18 GMAG along with lessons learned from the GOES-16/17 MAGs. The GOES-R series magnetometer instrument includes two magnetometer sensors (inboard and outboard) mounted along a boom extended from the spacecraft. As with the previous magnetometers, the GMAG sensors are three-axis fluxgates sampling the geomagnetic field at 10 samples/second, with the data low-pass filtered with a 2.5 Hz cut-off. On-orbit analysis demonstrates that the GOES-18 GMAG is a highly stable instrument showing little variations between the inboard and outboard sensors either diurnally or over multiple days. A nearly 2.5 months collocation between GOES-18 and GOES-17 (136.8°W and 137.2°W) allowed direct cross-satellite comparisons that was unprecedented for GOES satellites. Differences between the on orbit performance of the GMAG and MAG sensors are attributed to thermal stability issues observed on the GOES-17 MAG (also observed on the GOES-16 MAG). The cross-satellite analysis during the collocation interval, along with inboard/outboard sensor comparisons and comparisons to models, suggests that the GOES-18 GMAG meets the NOAA mission requirement of ±1 nT accuracy, excluding arcjet firing periods. Arcjet firing periods were also excluded in performance analysis for GOES-16/17.

Keywords GOES satellites · Magnetometer · Magnetosphere · Space weather

Extended author information available on the last page of the article

1 Introduction

NOAA's Geostationary Operational Environmental Satellite-R (GOES-R) series are the most recent generation of geostationary weather satellites for the United States. They consist of four satellites - GOES-R, S, T and U. The 3rd satellite in the GOES-R series, GOES-T, was launched on March 1, 2022 from Cape Canaveral Space Force Station, Florida and was renamed GOES-18 after launch. GOES-R, launched on November 19, 2016, (called GOES-16 on orbit) and has been the operational GOES-East spacecraft at 75.2°W since December of 2017. GOES-S was launched on March 1, 2018 and was operational at the west position of 137.2°W from February 2019 to January 2023, when it was replaced by GOES-18. GOES-U is currently slated for launch in 2024 and will be designated GOES-19 after reaching geostationary orbit. All GOES satellites orbit at geostationary orbit or, 6.6 Earth radii (R_E), and complete one orbit of Earth every 24 hours. At the time of this publication, GOES-18 has completed on-orbit post-launch testing (PLT) and post-launch product testing (PLPT) and was delivered from NASA to NOAA for weather operations in January, 2023.

The original magnetometer (MAG) instruments for all GOES-R series satellites were designed and built by Macintyre Electronic Design Associates (MEDA) Inc. and referred to as the MEDA MAGs. However, as a result of issues observed in the MAG data from GOES-16 (Loto'aniu et al. 2019) and GOES-17, a decision was made by the GOES-R program to replace the flight magnetometers for the next two GOES-R series spacecraft. It should be noted that the GOES-16/17 magnetic field observations met NOAA requirements, albeit with waivers to the original requirements.

The new magnetometers, GMAG, were built by the NASA-Goddard Space Flight center (GSFC) Planetary Magnetospheres Laboratory in Maryland. The GSFC Planetary Magnetospheres Lab has a long history of building science-grade space magnetometers for spacecraft missions including Voyager 1 and 2, Wind, ACE, MAVENS, DSCOVR and Solar Probe Plus. They also built the fluxgate magnetometers for the Van Allen Probes magnetospheric mission (Kletzing et al. 2013).

Science objectives for the GOES-R series magnetic field observations have previously been discussed by Loto'aniu et al. (2019). In this paper, Sect. 2 describes the GMAG requirements including a brief discussion of changes made for GMAG as result of lessons learned from the use of GOES-16/17 MAGs. Section 3 presents a short summary of the GMAG pre-launch calibration, Sect. 4 presents post-launch calibration/validation results and in Sect. 5 we give conclusions.

2 The Goddard Magnetometer Instrument Requirements

The GMAG sensor design is based on the magnetometers onboard the Juno mission (Connerney et al. 2017), MAVEN (Connerney et al. 2015) and Solar Probe Plus (Bale et al. 2016) magnetometers. The top panel of Fig. 1 shows a cartoon image of the GMAG sensor uncovered (left) and covered (right). As with the previous GOES-R series satellites, the GOES-18 GMAG system consists of two, three-axis, ring-core fluxgate magnetometers mounted on an 8.5 m boom that extends out from the spacecraft. Separating the magnetometers from the spacecraft bus decreases the spacecraft magnetic signature at the sensors. The first magnetometer, denoted as the inboard sensor (IB), is located 6.35 m from the spacecraft along the boom and the second magnetometer, the outboard sensor (OB), is located on the end of the boom at 8.55 m. The reader should refer to Loto'aniu et al. (2019) for details of requirements common to all the GOES-R series magnetometers, including figures within showing the locations of the sensors on the boom.
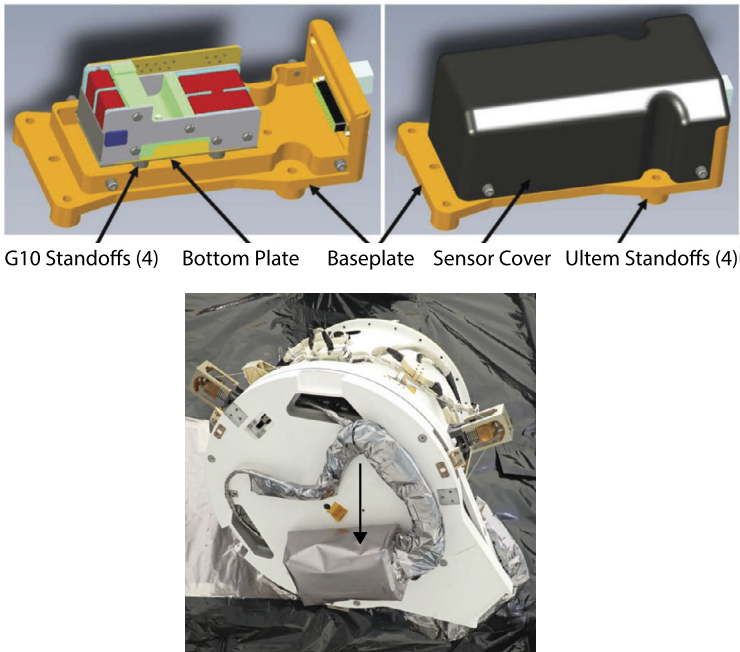
G10 Standoffs (4)   Bottom Plate   Baseplate   Sensor Cover   Ultem Standoffs (4)

Fig. 1 Top image shows a cartoon of the GMAG sensor without cover (left) and with cover (right). Bottom image shows the outboard sensor (noted with black arrow) mounted on the boom in the stowed position with the sensor and harness covered in thermal blanketing

Table 1 GOES-18 Magnetic Field Observational Requirements

Parameter	Requirements[a]
Geomagnetic Field	3-axis vector observation in-situ
Accuracy	1.0 nT/axis
Sample Rate	10 (originally 2) samples/second/axis
Orthogonality	0.5° (originally 0.1°)
Noise	0.3 nT
Noise (transients)	1 per hour for < 5 seconds
Range	±512 nT
Quantization Resolution	0.016 nT

[a]The values stated are in one or either of the NOAA GOES-R Series Level I Requirements Document (LIRD) and the NOAA Mission Requirements Document (MRD). The official NOAA sample rate is 2 samples/second, and 10 samples/second is the implemented value and found in the GOES-R Series Data Book [see www.goes-r.gov for LIRD, MRD and data book documents].

The GOES-18 magnetic field observational requirements are shown in Table 1, which are the same as the pre-waiver requirements for GOES-16/17 magnetometers. The noise requirement is defined in the time domain as 0.3 nT + 1 transient allowed per hour lasting 5 seconds. A transient in this respect means any unwanted or artificial noise signal above the 0.3 nT requirement. In implementing this requirement the accommodation was 0.1 nT to

Table 2 GMAG Ground Performance

Parameter	Ground Performance
Power Consumption	<5 Watts Total
Mass	Sensor Unit ≤0.5 kg, Electronics Units ≤2.15 kg
Range	±512 nT (nominal operations)
Noise	∼0.03 nT/$\sqrt{\text{Hz}}$ at 1 Hz
Frequency Response	2.5 Hz cutoff (anti-alias Butterworth filter)
Sample Rate	10 Hz

instrument noise and 0.2 nT to spacecraft noise, while in the spectral domain the requirement was validated up to the 2.5 Hz Butterworth filter cutoff but quoted at 1 Hz.

Lessons learned from GOES-16 (Loto'aniu et al. 2019) were applied to GOES-17, which reduced spacecraft magnetic interference and resulted in providing additional instrument thermal blanketing for increased thermal stability. The magnetometers built for GOES-16 and GOES-17 were found to be thermally unstable due to unexpected temperature gradients across the sensors. The analog to digital conversion (ADC) was also improved for GOES-17 through better circuit design. Although these changes significantly increased the quality of the GOES-17 magnetometer observations relative to GOES-16, the observational requirements still required a waiver for the GOES-17 MAGs as thermal stability issues, although much improved, persisted. For GOES-18, engineering redesigns were implemented to further improve thermal stability of the instrument and these changes included the following:

- New Sensor Units (SUs)
- New Electronics Units (EUs)
- Heaters placed on base exterior of GMAG EUs
- Spacers added to GMAG EU base to thermally isolate the EUs from spacecraft
- Spacers place at GMAG SU bobbin base to thermally isolate it from SU cover base, as shown in Fig. 1
- Spacers placed on the outside of the OB GMAG SU cover base to thermally isolate SU from boom tip plate, as shown in Fig. 1
- Heaters placed on the outside of GMAG SU cover positioned on three sides with thermal spreaders and 12 layer patch blankets over the heaters
- Additional thermal blanketing added, as shown in the bottom panel of Fig. 1
- Intensive ground thermal testing campaigns

Table 2 shows basic GMAG performance parameters based on ground tests. All the ground tests showed the GMAG sensors meeting instrument level pre-launch requirements including the 0.1 nT noise allocated to the instrument. One of the differences between GMAG and the previous GOES-R magnetometers is that GMAG has three measurement ranges, which cover ±128 nT, ±512 nT and ±65536 nT. The ±512 nT range shown in Table 2 is used for nominal on-orbit operations, while the ±128 nT range is useful for diagnostics and the wider ±65536 nT range can be used during coarse ground testing because it covers the full range of Earth's magnetic field on the ground. Multiple ranges allow for the best testing depending on the sensor's magnetic environment.

3 Ground Calibration

The GOES-18 GMAGs underwent extensive ground calibrations to determine initial values for sensor zero-level bias, scale factors, misalignment and temperature dependency. The

Table 3 Calibration maneuver results of sensor bias estimates in nT

Maneuver date	Kp	IBx	IBy	IBz	OBx	OBy	OBz
29 June, 2022	2	3.13	−2.54	7.66	4.28	−1.52	−2.25
6 July, 2022	1+	3.14	−2.48	7.83	4.19	−1.57	−2.47
Std. Dev.		0.23	0.27	0.32	0.26	0.24	0.33
Pre-launch measurements[*]		1.16	1.03	−3.07	−1.29	−1.63	3.52

[*]Determined from ground testing

procedures for determining these values are similar to those used for previous GOES-R magnetometers. The ground calibration campaign for the GOES-16 magnetometers, including transfer equations, are described by Loto'aniu et al. (2019). For details of the methodologies used to determine GMAG calibration values useful references include Connerney et al. (2015), Leinweber et al. (2008), Acuna (1978), McPherron and Snare (1978), and Risbo et al. (2003). Precise ground calibration values are usually determined by placing the instrument in a coil that nulls Earth's magnetic field, allowing for isolated magnetics testing. The GOES-R magnetometers used the NASA Goddard Space Flight Center M.H. Acuna test facility (Vernier et al. 2004) for this procedure.

The coordinate systems relevant to the GOES-18 magnetometers can be found in Loto'aniu et al. (2019, 2020), with the frames common for all GOES-R magnetometers. Magnetometer data are recorded in the internal sensor, uncalibrated and non-orthogonal, frame. The data are then calibrated, orthogonalized and rotated into other frames. One of the frames important to this study is the Earthward-Poleward-Normal (EPN) frame, where the P-axis is defined as normal to the orbit plane, E is the Earthward (nadir) direction, and N completes the right-handed system (E × P) and points eastward.

Zero offset determination involves rotating the magnetometer sensor about its horizontal and vertical axes while external magnetic fields are nulled by the coil system. The GMAG team observed offset repeatability to within ∼0.1–0.2 nT. In Table 3, the bottom row shows the ground-based determined GMAG zero offsets. The scale factors for GMAG are range-dependent, and multiple measurements were taken in each range to show repeatability. All the measured scale factors fell within 0.5% of idealized values.

Two independent methods were used to determine sensor axis orthogonality matrices, the thin shell and MAGSAT methods (Acuna 1978; Risbo et al. 2001, 2003), with differences in results between the methods less than 0.1%. The GMAG noise, which represents the sensitivity limit of the magnetometer, was determined by taking the power spectral density of the GMAG data. The GOES-18 analog to digital convertor samples at 320 Hz, then using a simple boxcar averages down inside the GMAG electronics logic to provide the vector samples at 10 Hz telemetry. Overall, ground calibration testing showed that GMAG met all instrument requirements. In-flight, some parameters such as offsets and noise levels need to be measured again as the contribution from the spacecraft has to be subtracted, and launch can cause changes in instrument calibration (See Sect. 4).

3.1 Temperature Dependency

Geostationary orbit can be a particularly harsh radiation environment for satellites and instruments. In this region, solar wind variations cause changes in Earth's ring current and radiation belts and can create dangerous levels of energetic electrons that can lead to issues

such as surface charging, deep dialectric charging and damage to electronic systems. In addition, thermal stability issues observed on GOES-16, and to a lesser extent on GOES-17, resulted in GOES-18 magnetometer changes that included an emphasis on improved thermal design, as discussed in Sect. 2, and extensive ground thermal stability testing. The GMAG Sensor Units (SUs) and Electronics Units (EUs) underwent testing at the Acuna magnetics test facility. Long-Term Stability Test (LTST) was also performed at the test facility between November 1, 2019 and December 13, 2019. During this period the GMAG was powered on and the EUs and SUs were intermittently heated to different temperatures while data were collected and temperature dependent errors were estimated for the EUs and SUs.

The error from temperature variations can be estimated from the difference in magnetic field observations between the heated EU (or SU) and the EU (or SU) left at ambient temperature. For the EUs, the worst-case scenario on-orbit was predicted to show a ± 0.04 nT diurnal variation for all three axes of the OB sensor, with smaller values expected for the IB sensor. For the SUs, on-orbit errors due to temperature variation was predicted to be at worse ± 0.11 nT for the y-axis of the IB sensor and ± 0.16 nT for the z-axis of the OB sensor. Long-term testing results suggest that GMAG should show a stable, predictable change in response to the varying thermal environment on-orbit. Thermal stability testing was repeated on-orbit by changing the operating temperature, or set point, of the sensors with results presented in Sect. 4.2.

4 On-Orbit Calibration

On-orbit, GOES-18 GMAG was turned on and then the boom was deployed on 23 March, 2022. Post-launch testing (PLT) and on-orbit calibration periods were split between two geostationary longitudinal locations before the spacecraft reached its final operational position. From 23 March to 16 May, 2022, GOES-18 was parked at 89.5° West geographic longitude for the first phase of PLT. After a drift period of approximately two weeks, the spacecraft relocated to 136.8° West geographic longitude for the second phase of PLT. On 5 July, 2022, GOES-18 underwent an approximately three week "nudge" to 137.0° West geographic longitude where, as of writing, it operates as GOES-West. This section will present results from the post-launch calibration tests.

4.1 Boom Deployment and Offset Determination

The boom and deployment mechanisms are the same for all GOES-R series satellites. The GOES-18 GMAG boom deployment data is shown in the top panel of Fig. 2. The GOES-18 IB sensor reached its on-orbit stop position first, after about 30 seconds, followed by the OB sensor 15 seconds later. Rotational unwinding of the boom causes oscillations in the field measurements until the sensors reached final positions. The small field fluctuations near 12:23:55 UT, which dampen away in minutes, are caused by vibrations when the boom reaches its full extent. During deployment, the sensors showed an expected $1/r^3$ decrease with distance in the contribution of the spacecraft field. The spikes observed at the start of deployment are caused by the sensors moving out of the canister past regions of high magnetic contamination before the boom extends away from the spacecraft and the total magnetic field reduces as expected.

On GOES-16, after completion of boom deployment, the magnetometer data showed an unexpected 10's of nT offset (Loto'aniu et al. 2019), most likely due to magnetic contamination from magnetic tape placed near the MAG sensor which was not removed before launch.
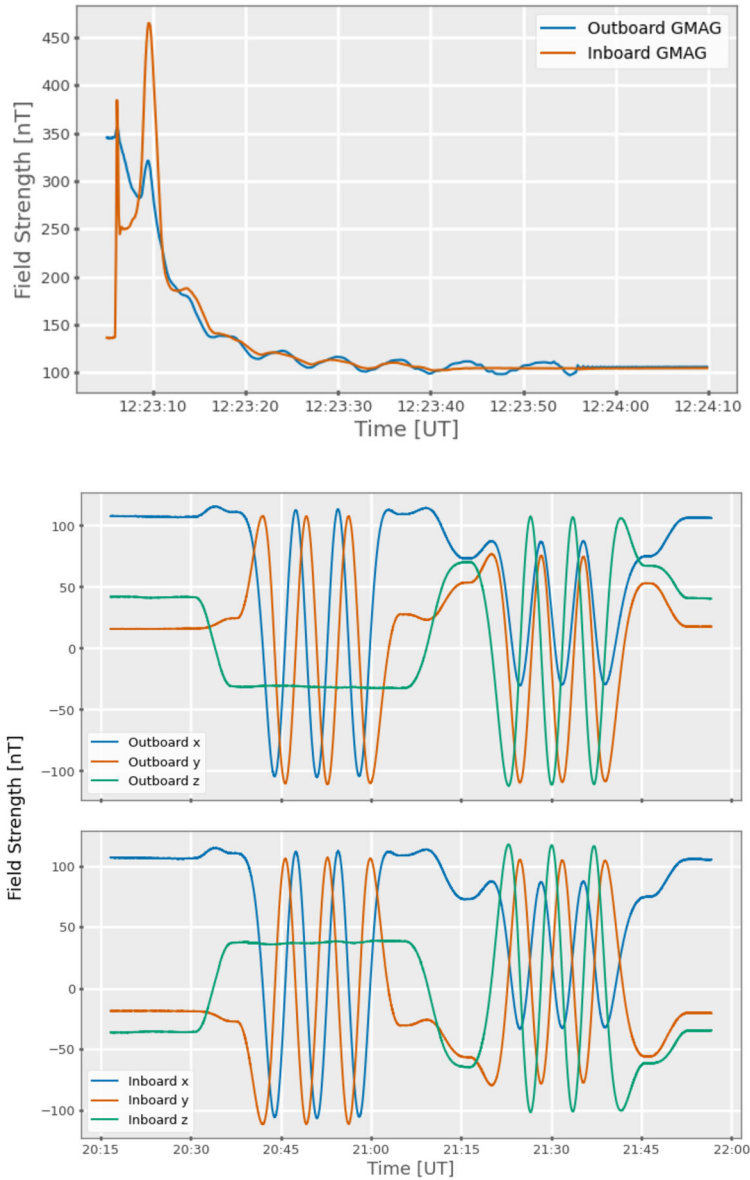
Fig. 2 The top panel shows the total magnetic field strength measured by the GOES-18 GMAG IB and OB sensors in sensor frame coordinates during boom deployment on 23 March, 2022. The bottom two panels show the geomagnetic field strength measured by the IB and OB sensors in three components in the sensor frame during the three-revolution calibration maneuver on 29 June, 2022

A re-emphasis on magnetic cleanliness as part of lessons learned meant this large contamination was not observed on GOES-17 (results not shown here) or GOES-18. It should be noted that on GOES-16, this particular contamination was mostly DC and therefore removed after the GOES-16 magnetometer offsets were applied (Loto'aniu et al. 2019).

In determining GOES-18 GMAG on-orbit offsets, a series of spacecraft rotational slews about two axes were undertaken, similar to the maneuvers done for GOES-17. The bottom two panels in Fig. 2 show an example of the measured field of the OB and IB sensors during three 360° spacecraft revolutions about two axes. Rotating the spacecraft creates a sinusoidal signal in the magnetic field measurements of the rotating axes (in the sensor coordinate frame). The other variations are mainly due to spacecraft attitude re-orientation. Spacecraft rotations allow an estimate of the offsets because during rotation the ambient field will be observed to rotate in the sensor frame while the sensor offsets and spacecraft field do not.

However, since the ambient magnetic field naturally varies and the axes of rotation do not align with the sensor component axes, a linear least-squares interpolation method is used to approximate the background field and determine zero-level offset and alignment biases. The methodology employed for GOES-18, which is currently being written as a separate paper, is an improvement over that of GOES-16, which did not estimate the background field. Further improvements were made by using a spherical interpreter to interpolate between spacecraft quaternion samples, which provides an improved profile of spacecraft position during the maneuver.

Two sets of calibration maneuvers were performed. The first, on 29 June, 2022, included three full 360° revolutions about two axes, while the second, on 6 July, 2022, was a one revolution maneuver about the same two axes. Table 3 shows that estimated offsets were similar for the two maneuvers. Both maneuvers occurred during quiet space weather conditions (Kp ≤ 2 during the slews). Offsets from ground calibrations are also shown in Table 3, which are significantly closer to the on-orbit calculations than those for GOES-16 (Loto'aniu et al. 2019). The largest offset is in the IB z-axis component, which was also the largest on GOES-16 and GOES-17. The GOES-17 and GOES-18 IB z-axis values were similar. However, the GOES-16 IB z-axis offset was a factor of 10 higher in absolute terms due to the previously mentioned DC offset contamination observed in GOES-16 magnetometer data.

Results from the three revolution maneuvers were applied to magnetometer data products because the additional rotations increase confidence in repeatability compared to the single revolution maneuver. Figure 3 shows example GMAG OB-IB differences without (top panel) and with (bottom panel) biases applied for each component. Applying the corrections significantly decreases the difference between the OB and IB measured field values. Sensor differences over time provide a particularly useful indicator of the stability of the sensors. Ideally, the calibrated sensors would have a difference of zero nT. Throughout the day shown in Fig. 3, the largest sensor difference is for OB-IB z-axis, up to ∼6 nT. After corrections, the GOES-18 GMAG sensor differences for all components is below 1 nT. For NOAA-NCEI publicly available GOES-18 GMAG data products, biases are applied to observations made after 8 August, 2022.

4.2 Thermal Stability and Set Point

Magnetometers orbiting at geostationary altitude encounter a thermal environment that changes with changing solar illumination as the spacecraft orbits Earth. This includes periods of spacecraft shadowing from the Sun and varying thermal conditions due to seasonal changes. For the GOES-R series, it was decided to maintain the magnetometers at a constant operating temperature or set point. This set point is maintained using thermal blanketing and heaters with a zero degree dead-band temperature range, meaning heaters are activated if there is any change in sensor temperature below the set point. However, in reality the extreme thermal environment at geostationary orbit will still cause some variations in temperature across the sensors.
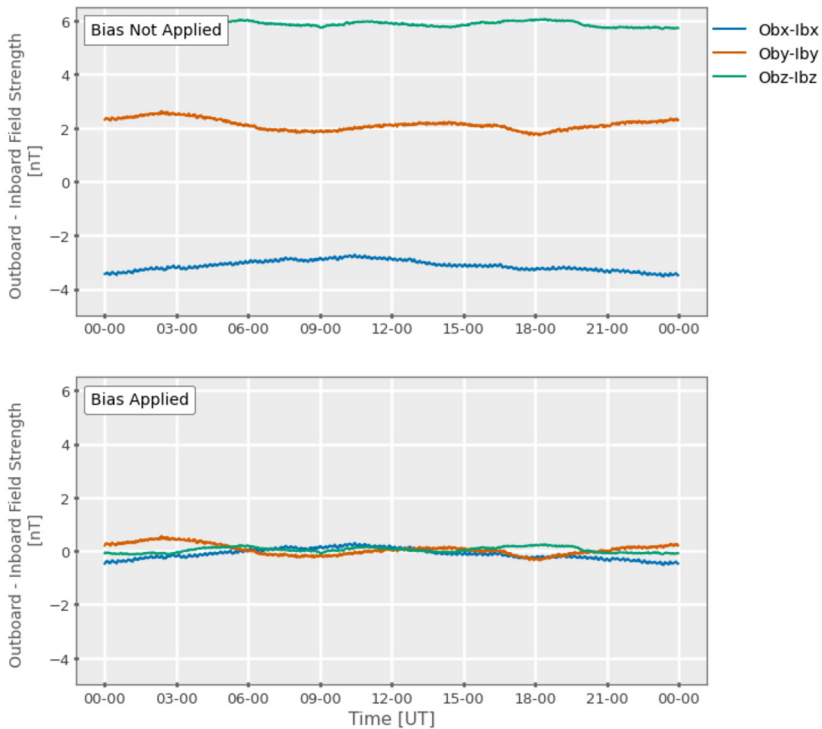
Fig. 3 Example data comparing IB and OB sensor differences without (top panel) and with (bottom panel) the calibration maneuver zero-offset and alignment bias corrections applied. Data from 5 July, 2022 is used to compute the difference in field strength measured by each sensor in three components

Pre-launch calibration determined an optimal set point temperature of 23 °C. Post-launch, the set point was re-established using thermal stability tests. This involves stepping through the set point of one sensor (from 20 °C to 30 °C and back again), while the set point of the other sensor is kept constant. At each set point temperature the change in OB-IB was observed. The test was then repeated for the other sensor. Test results for each axis for the IB are shown in Fig. 4, where the x-axes are the set point temperatures and y-axes are the OB-IB values at each set point. The line of best fit is also shown along with linear regression equation and R^2 value. The value represented by the big dot at 30 °C in the Z-axis plot was not used in the regression analysis because it is out of family with the other values and assumed to be an anomalous reading. For the OB sensor (results not shown), except for one anomalous reading, the spread in OB-IB values over the entire set point temperatures were no more than about ±0.1 nT, smaller than the spread of values observed when the IB sensor was tested.

Overall, the tests show no compelling reason to change the GOES-18 GMAG sensor set point temperature from the pre-launch value of 23 °C. Using a 0 °C dead band, the spread of the data points from the line of best fit in Fig. 4 indicates that the GMAG sensor OB-IB values should vary by no more than about ±0.2 nT throughout the day due to diurnal thermal environment changes. A constant operating temperature is also used for the GOES-16 and GOES-17 sensors. However, the on-orbit GOES-16 MAG sensor differences can be as high as 10 nT or more over a day even after biases were applied (Loto'aniu et al. 2019),

Fig. 4 Results of GOES-18 GMAG IB set point temperature tests from May 2022. Shown are OB-IB sensor differences for each axis after the IB set point temperature changes. Included are lines of best fit, linear regression equations and R^2 correlations
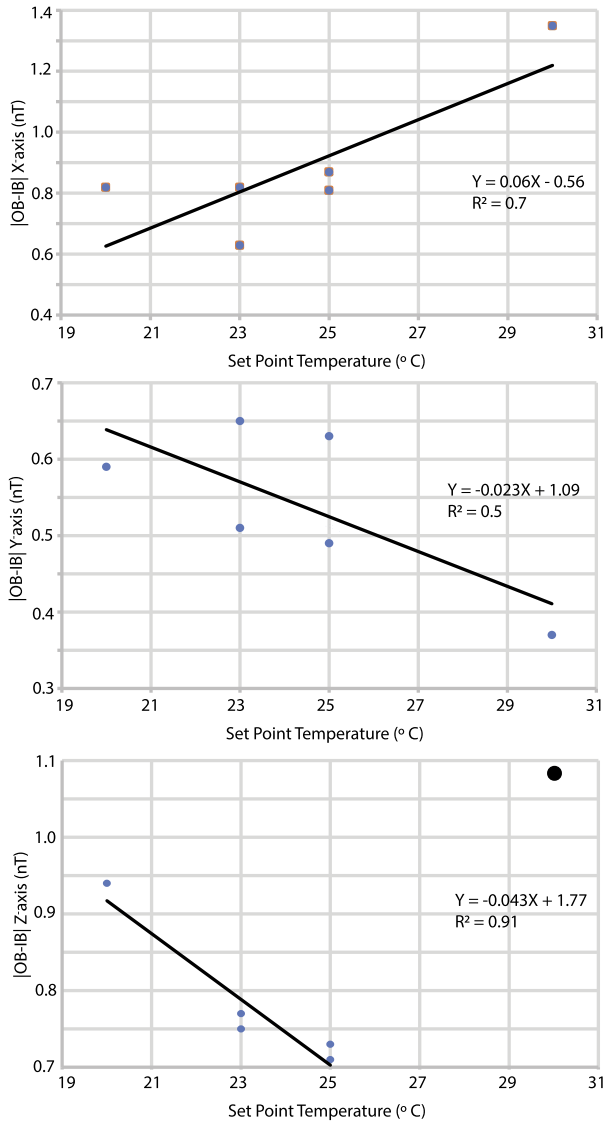
as shown in the following section. It should be noted that there has been considerable work undertaken to develop a correction algorithm for the solar dependent thermal anomalies observed on GOES-16 using machine learning methods (Inceoglu and Loto'aniu 2021).

4.3 Initial Cross-Satellite and Model Comparisons

Figure 5 shows full resolution OB-IB data for one day from the GOES-16 MAG (lower panel), GOES-17 MAG (middle panel) and GOES-18 (top panel). Improvement in the magnetometer sensor data quality with each GOES-R satellite is clearly visible. The GOES-16 MAG data exhibits significant variation throughout the day (as high as >10 nT) in response to the changing diurnal thermal environment. GOES-17 MAG shows great improvements
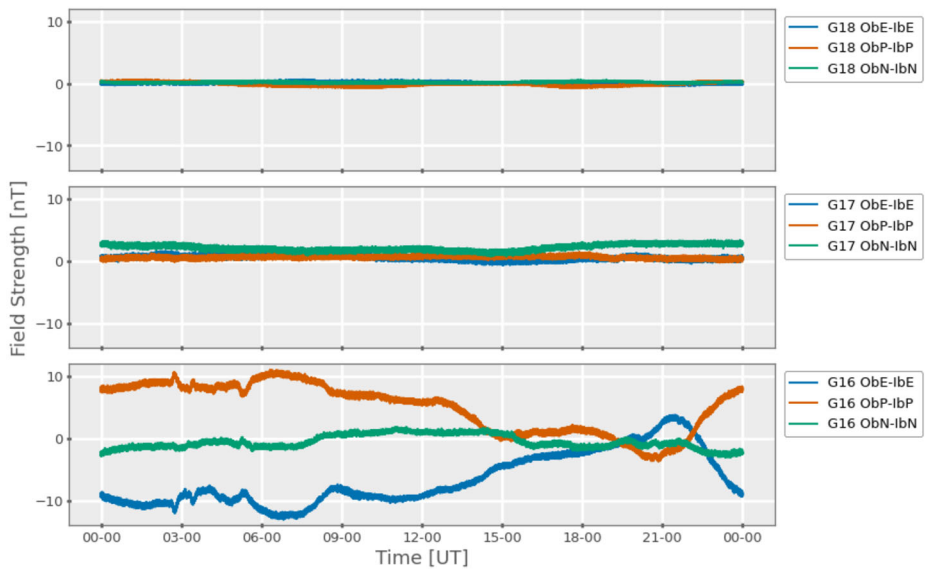
Fig. 5 Comparison of OB - IB sensor differences in three components for GOES-16 (bottom), -17 (middle) and -18 (top). All data sets have calibration zero-offset and alignment corrections applied and were measured on 14 August, 2022

with less daily variation of about 2 nT. The GOES-18 GMAG shows less than <1 nT variation. The GOES-18 GMAG shows less than <1 nT variation. In addition, the thickness of the time series curves are thinner for GOES-18 GMAG indicating less noise compared to GOES-17 or GOES-16 MAGs. The GMAG sensors are significantly more stable than either GOES-16 or GOES-17. We believe the better results for GOES-17 compared to GOES-16 are due to the extra thermal blanketing around the GOES-17 sensor and the lack of magnetic tape placed near the sensor, which on GOES-16 caused large contamination signals. Although the magnetic contribution from the tape left on GOES-16 was mainly DC (Loto'aniu et al. 2019), the tape may have soft magnetic properties which would cause unwanted variations throughout the day.

During the second phase of PLT GOES-18 was located at 136.8°W geographic longitude, close to GOES-17 located at its operational position of 137.2°W geographic longitude. This period of close proximity, referred to as co-location, provided a unique opportunity to compare magnetic field measurements from GOES-17 to GOES-18. Analysis comparing field measurements of two satellites often requires removing the effect of longitudinal differences by subtracting magnetic model field values calculated at each satellite location. With such close proximity during co-location, model subtractions were not necessary.

However, it is important to note that comparisons between the GOES-17 and GOES-18 even at co-location are subject to inaccuracies in both the GOES-17 and GOES-18 magnetometers. Figure 6 shows daily IB-OB time series data in EPN coordinates for each satellite overlaid for 1.5 months during co-location, excluding times of thermal testing (on GOES-17) or arcjet firings (see Califf et al. 2020b). Daily profiles for GOES-18 are much more stable (flat) than those of GOES-17, and have significantly less spread between days. The mean plus 1-σ over the 1.5 months of co-located data are shown in Table 4. There is an obvious offset seen in the GOES-17 MAG N-component IB-OB that has a mean of −2.1 nT, while the GOES-18 GMAG means do not reach 0.1 nT on any component. The σ values for
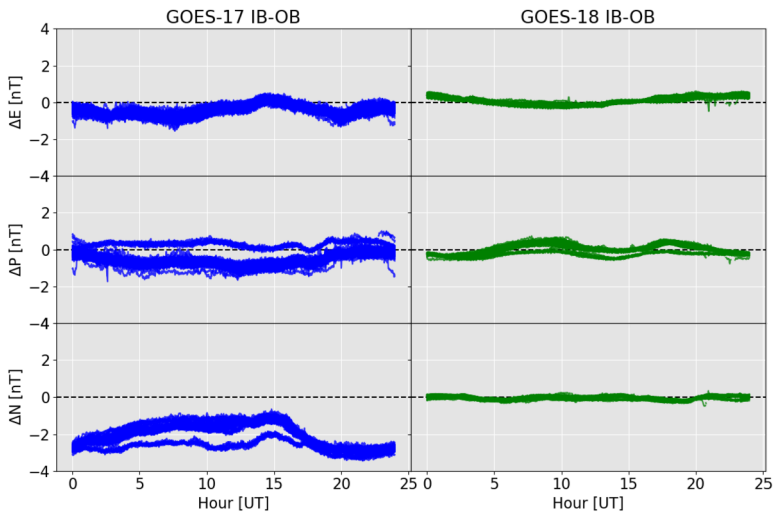
Fig. 6 IB-OB daily sensor differences in three components (EPN coordinate frame) for GOES-17 (blue) and GOES-18 (green), overlaid for 1.5 months. Differences were taken during co-location when the spacecrafts were less than 0.5 degrees longitude apart. Any instances of thermal testing, high (>2) Kp or arcjet burns are excluded

Table 4 GOES-18 and GOES-17 mean IB-OB $\pm\sigma$ over 1.5 months during satellite co-location in EPN coordinates, discounting periods of thermal testing or arcjet firings

Satellite	E	P	N
GOES-17 [nT]	-0.43 ± 0.30	-0.47 ± 0.44	-2.10 ± 0.62
GOES-18 [nT]	0.09 ± 0.21	-0.00 ± 0.30	-0.01 ± 0.11

GOES-17 are also higher than GOES-18 and in both cases part of this diurnal variation is probably due to the changing thermal conditions through the day.

Although co-location provides a great opportunity to directly compare GOES-17 MAG to GOES-18 GMAG, the GOES-17 observations should not be used as the primary numerical indicator of the GOES-18 GMAG accuracy. The GMAG sensors are thermally more stable than the MAGs on GOES-16/17. Furthermore, on July of 2021 GOES-17 experienced an anomaly which resulted in all instruments entering safehold. After restarting from safehold mode, there was a slight shift in the MAG sensor biases. The cause of the bias shift is unknown, and this additional bias remains, albeit at a lower amplitude. This shift in the GOES-17 bias is a likely contributing factor in the offsets observed in the GOES-17 IB-OB. It is suggested that a better indication of accuracy is the sensor differences shown in Fig. 6, which clearly indicates that the GMAG sensors are more stable and have a mean IB-OB very close to zero nT.

In addition to inter-satellite comparisons, Fig. 7 shows GOES-18 field measurements plotted over the Tsyganenko (1989) (T89) and Tsyganenko and Sitnov (2005) Storm Time (TS04) magnetic field models for a period just over 2 weeks in November 2022. The accuracy of the models will decrease if the quality of the input solar wind data to the models are poor. For this study, model inputs are the Deep Space Climate Observatory (DSCOVR) solar wind parameters, which have been propagated from Larange point 1 (L1) to Earth's bow
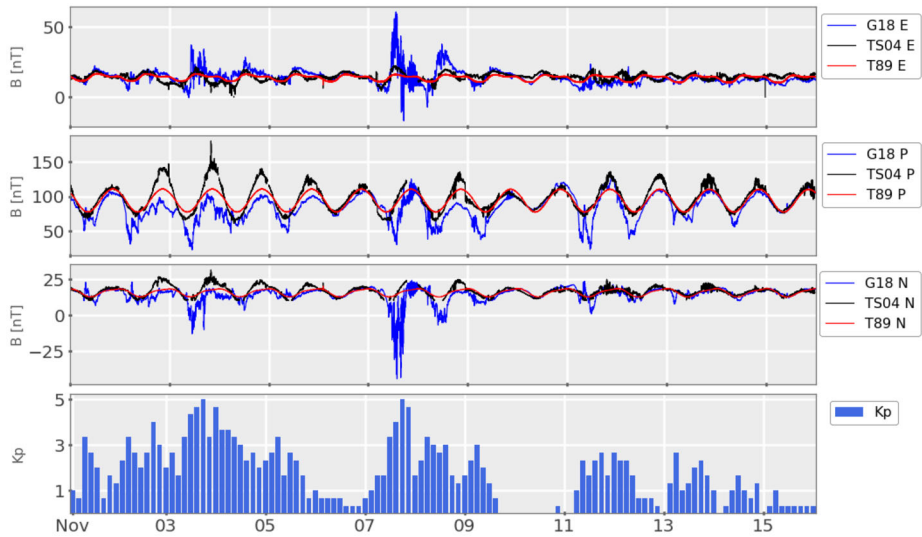
Fig. 7 Example comparisons of GOES-18 measured magnetic field data with output from Tsyganenko 1989 and Storm Time 2004 (TS89 and TS04) models and Kp index. All Kp values, including non-quiet time, are included although it is noted that models were run with quiet time parameters

shock. This dataset is known to have some issues with the plasma data depending on solar wind speed (Loto'aniu et al. 2022). Model comparison allows an assessment of the general trends, but should not be used for assessing the quantitative accuracy of the GOES-18 GMAG. The general trend of the GOES-18 GMAG data follow the field models. However, during low geomagnetic activity conditions (Kp ≤ 2) comparisons between the models and GMAG data are closer.

4.4 Data Issues and Magnetic Contamination

4.4.1 Arcjet Contamination

The arcjets are used for North-South station keeping of the GOES-R satellites. Arcjet contamination is a known problem in the GOES-R series magnetometer data (Loto'aniu et al. 2019; Califf et al. 2020b), which can cause a large up to 20 nT step in magnetic field values for the duration of the firing. Figure 8 shows an example of this contamination in the GOES-18 GMAG data. As with the GOES-16 and GOES-17 MAGs, the arcjet effect is seen in both sensors and in all three components. Arcjets firings occur approximately every 4 days for approximately 90 minutes but there are occasional shorter duration bursts, and the same configuration of arcjets may not be used in all firings (such as dealing with power supply or different station keeping).

There is a correction implemented in the ground processing system that removes some of the arcjet effect (Califf et al. 2020a) and this correction is shown in Fig. 8. However, the correction is only valid for particular arcjet firing configurations and is not valid for the beginning and end of the firing period, as seen by large spikes. Work is ongoing to create additional potential improvements to the correction algorithm. Current corrected data products should be used with caution as the spikes can be misinterpreted. There is an arcjet firing flag in all GOES-R magnetometer data products. It is recommended that for science
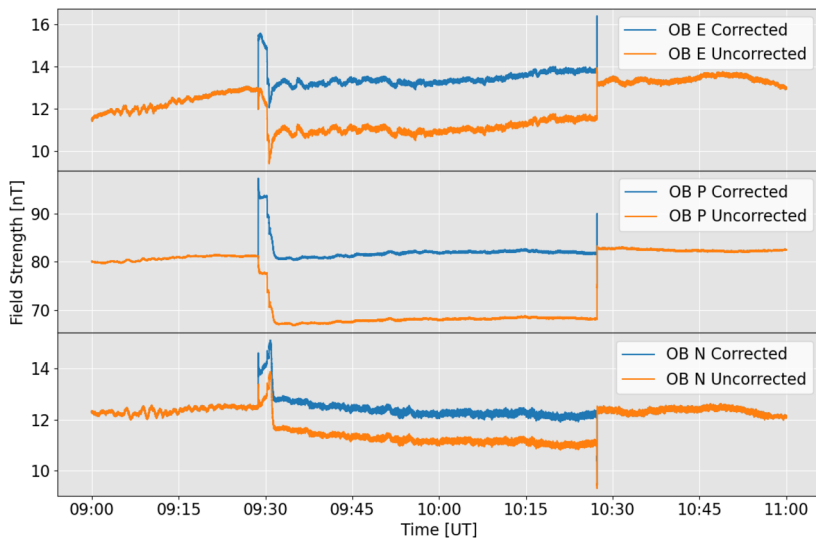
Fig. 8 GOES-18 OB measured field data in three components (EPN coordinate frame) during an arcjet firing. The orange lines show the original, uncorrected arcjet effect (sudden step of up to 20nT) while the blue lines show the corrected field data

users, the arcjet firing periods should be flagged and not used in scientific research unless the research is about the arcjet effects.

4.4.2 Noise Levels

The noise requirements were validated both in the time and frequency domain. In the time domain we validate the noise as an RMS value taken over an hour or more and selecting multiple days when Kp is low. In the frequency domain, variable FFT lengths were used, and the noise requirement validated up to the 2.5 Hz Butterworth filter. Analysis was undertaken over multiple days where Kp was low. Figure 9 shows a comparison of dynamic (top panels) and static (bottom panels) magnetic field power spectral density (PSD) for the same day from the GOES-18 and GOES-17 magnetometers. Overall background noise across all frequency ranges is lower on GOES-18. The lines and bright U/V shapes in the dynamic spectra are due to reaction wheels. Spacecraft reaction wheel signatures are commonly observed in space-based magnetometer data because the rotation periods of the wheels can vary over a wide range, often falling within the instruments' measuring bandwidth. This contamination is observed on all GOES-R series magnetometers (Loto'aniu et al. 2019).

In the example static spectrograms, the drop-off in power due to the 2.5 Hz Butterworth filter is observed in both spectra. The spikes in power between about 0.2-0.6 Hz are due to reaction wheel noise, considering that the contamination for GOES-18 is similar to that observed on GOES-16/17. However, the baseline background noise level is clearly lower by an order of magnitude in GOES-18 and below the observational noise requirement. The noise when including spacecraft reaction wheels is below the 0.3 nT (PSD $\sim$ 0.1 nT^2/Hz) observational requirement, while without reactions wheels it is below the 0.1 nT (PSD = 0.01 nT^2/Hz) instrument allocation. Results for time domain RMS values were similarly within requirements. The lower noise level on the GOES-18 magnetometer enhances the possible science studies of geophysical interest within the GMAG bandwidth, including the study of low amplitude Ultra Low Frequency (ULF) waves.
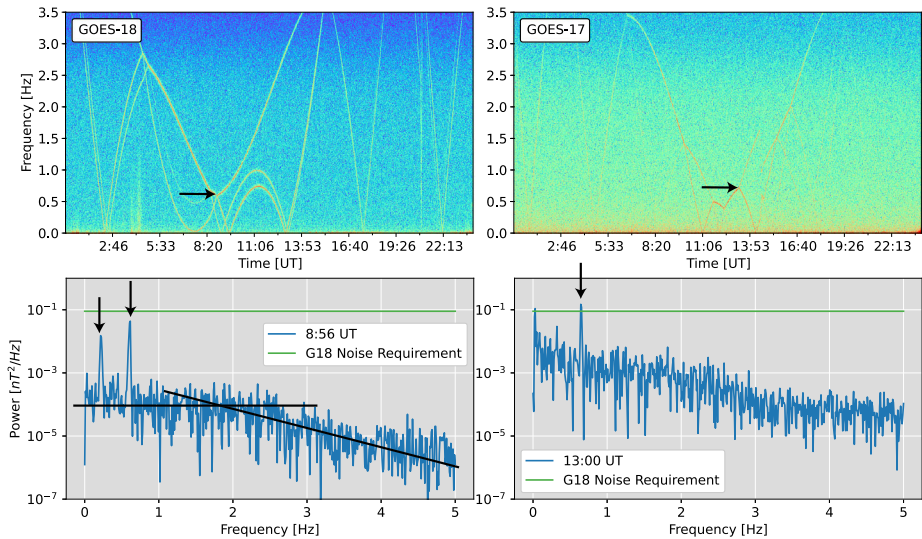
Fig. 9 (top row) GOES-18 OB x-component daily spectrogram compared to GOES-17 for the same day. The thin lines and U shaped signals in the spectra are due to reaction wheel interference and noted with black arrows. (bottom row) Static spectrogram taken around 08:56 UT for GOES-18 and 13:00 UT for GOES-17. The spikes in the static spectra indicate contributions of the reaction wheels (black arrows). The effect of the 2.5 Butterworth filter is seen by the change of slope using black lines

5 Conclusions

The new NOAA GOES-18 GMAG sensors successfully incorporate lessons learned from the use of the magnetometers on GOES-16 and GOES-17. Ground and on-orbit calibrations have significantly reduced the effect of spacecraft fields and interference in the magnetometer observations. An unprecedented period of co-location between GOES-18 and GOES-17 allowed for direct comparison of the two sets of magnetometers. It was demonstrated that the GMAG sensors are not as susceptible to diurnal and long term variations, with GMAG showing up to 2 nT less variation than GOES-17. Comparisons to magnetic field model outputs generally match the profile of GOES-18 observations (for low Kp days). Cross-satellite comparisons, inboard/outboard sensor comparisons and comparisons to models suggest that the GOES-18 GMAG is within 1 nT relative accuracy, excluding arcjet firing periods. Data from the now operational GOES-18 are publicly available and incorporated into SWPC alerts and products.

Declarations

References

Acuna MH (1978) Magsat: Vector magnetometer absolute sensor alignment determination. Tech. Rep. No. 79648, NASA Goddard Space Flight Center

Bale SD, Goetz K, Harvey PR et al (2016) The FIELDS instrument suite for Solar Probe Plus. Space Sci Rev 204(1):49–82. https://doi.org/10.1007/s11214-016-0244-5

Califf S, Early D, Grotenhuis M, Loto'aniu TM, Kronenwetter J (2020a) Correcting the arcjet thruster disturbance in GOES-16 magnetometer data. Space Weather 18(1):e2019SW002347. https://doi.org/10.1029/2019SW002347

Califf S, Loto'aniu T, Early D, Grotenhuis M (2020b) Arcjet thruster influence on local magnetic field measurements from a geostationary satellite. J Spacecr Rockets. https://doi.org/10.2514/1.A34546

Connerney JEP, Benn M, Bjarno JB et al (2017) The Juno magnetic field investigation. Space Sci Rev 213(1):39–138. https://doi.org/10.1007/s11214-017-0334-z

Connerney JEP, Espley J, Lawton P, Murphy S, Odom J, Oliversen R, Sheppard D (2015) The MAVEN magnetic field investigation. Space Sci Rev 195(1):257–291. https://doi.org/10.1007/s11214-015-0169-4

Inceoglu F, Loto'aniu PTM (2021) Using unsupervised and supervised machine learning methods to correct offset anomalies in the GOES-16 magnetometer data. Space Weather 19(12):e2021SW002892. https://doi.org/10.1029/2021SW002892

Kletzing CA, Kurth WS, Acuna M et al (2013) The Electric and Magnetic Field Instrument Suite and Integrated Science (EMFISIS) on RBSP. Space Sci Rev 179(1):127–181. https://doi.org/10.1007/s11214-013-9993-6

Leinweber HK, Russell CT, Torkar K, Zhang TL, Angelopoulos V (2008) An advanced approach to finding magnetometer zero levels in the interplanetary magnetic field. Meas Sci Technol 19(5):055104. https://doi.org/10.1088/0957-0233/19/5/055104

Loto'aniu PT, Califf S, Redmon RJ, Singer HJ (2020) Magnetic field observations from the GOES-R series. In: Goodman SJ, Schmit TJ, Daniels J, Redmon RJ (eds) The GOES-R series: a new generation of geostationary environmental satellites. Elsevier, Amsterdam, pp 251–259. https://doi.org/10.1016/B978-0-12-814327-8.00021-4

Loto'aniu PTM, Romich K, Rowland W et al (2022) Validation of the DSCOVR spacecraft mission space weather solar wind products. Space Weather 20(10):e2022SW003085. https://doi.org/10.1029/2022SW003085

Loto'aniu TM, Redmon RJ, Califf S et al (2019) The GOES-16 spacecraft science magnetometer. Space Sci Rev 215:32. https://doi.org/10.1007/s11214-019-0600-3

McPherron RL, Snare RC (1978) A procedure for accurate calibration of the orientation of the three sensors in a vector magnetometer. IEEE Trans Geosci Electron 16(2):134–137. https://doi.org/10.1109/TGE.1978.294576

Risbo T, Brauer P, Merayo JMG, Nielsen OV, Petersen JR, Primdahl F, Richter I (2003) Ørsted pre-flight magnetometer calibration mission. Meas Sci Technol 14(5):674. https://doi.org/10.1088/0957-0233/14/5/319

Risbo T, Brauer P, Merayo JMG, Primdahl F, Balogh A (2001) Ørsted calibration mission: the thin shell method and spherical harmonics analysis. In: Balogh A, Primdahl F (eds) Ground and in-flight space magnetometer calibration techniques, ESA Special Publication, vol SP-490

Tsyganenko NA (1989) A magnetospheric magnetic field model with a warped tail current sheet. Planet Space Sci 37(1):5–20. https://doi.org/10.1016/0032-0633(89)90066-4

Tsyganenko NA, Sitnov MI (2005) Modeling the dynamics of the inner magnetosphere during strong geomagnetic storms. J Geophys Res 110. https://doi.org/10.1029/2004JA010798

Vernier R, Bonalsky T, Slavin J (2004) Goddard Space Flight Center Spacecraft Magnetic Test Facility restoration project. In: 23rd space simulation conference proceedings. NASA, Washington

Authors and Affiliations

Paul T.M. Loto'aniu[1,2] · **A. Davis**[1,2] · **A. Jarvis**[1,2] · **M. Grotenhuis**[3] · **F.J. Rich**[4] · **S. Califf**[1,2] · **F. Inceoglu**[1,2] · **A. Pacini**[2] · **H.J. Singer**[5]

✉ P.T.M. Loto'aniu
paul.lotoaniu@noaa.gov

[1]   Cooperative Institute for Research in Environmental Sciences, University of Colorado Boulder, Boulder, CO, USA

[2]   National Centers for Environmental Information, National Oceanic and Atmospheric Administration, Boulder, CO, USA

[3]   Goddard Space Flight Center, National Aeronautics and Space Administration, Greenbelt, MD, USA

[4]   Massachusetts Institute of Technology Lincoln Laboratory, Lexington, MA, USA

[5]   Space Weather Prediction Center, National Oceanic and Atmospheric Administration, Boulder, CO, USA